An unexpected role for TASK-3 potassium channels in network oscillations with implications for sleep mechanisms and anesthetic action

Daniel S. J. Pang[a,1], Christian J. Robledo[a,1], David R. Carr[a], Thomas C. Gent[a], Alexei L. Vyssotski[b], Alex Caley[a,2], Anna Y. Zecharia[a], William Wisden[c], Stephen G. Brickley[a], and Nicholas P. Franks[a,3]

[a]Biophysics Section, Blackett Laboratory, and [c]Cell Biology and Functional Genomics Section, Division of Cell and Molecular Biology, Imperial College, South Kensington, London SW7 2AZ, United Kingdom; and [b]Institute of Neuroinformatics, University of Zurich/ETH Zurich, Winterthurerstrasse 190, CH-8057 Zurich, Switzerland

Edited by Richard W. Aldrich, The University of Texas, Austin, TX, and approved August 24, 2009 (received for review June 29, 2009)

TASK channels are acid-sensitive and anesthetic-activated members of the family of two-pore-domain potassium channels. We have made the surprising discovery that the genetic ablation of TASK-3 channels eliminates a specific type of theta oscillation in the cortical electroencephalogram (EEG) resembling type II theta (4–9 Hz), which is thought to be important in processing sensory stimuli before initiating motor activity. In contrast, ablation of TASK-1 channels has no effect on theta oscillations. Despite the absence of type II theta oscillations in the TASK-3 knockout (KO) mice, the related type I theta, which has certain neuronal pathways in common and is involved in exploratory behavior, is unaffected. In addition to the absence of type II theta oscillations, the TASK-3 KO animals show marked alterations in both anesthetic sensitivity and natural sleep behavior. Their sensitivity to halothane, a potent activator of TASK channels, is greatly reduced, whereas their sensitivity to cyclopropane, which does not activate TASK-3 channels, is unchanged. The TASK-3 KO animals exhibit a slower progression from their waking to sleeping states and, during their sleeping period, their sleep episodes as well as their REM theta oscillations are more fragmented. These results imply a previously unexpected role for TASK-3 channels in the cellular mechanisms underlying these behaviors and suggest that endogenous modulators of these channels may regulate theta oscillations.

EEG | knockout | REM | theta | wavelet

If a sufficient number of neurons participate in network oscillations, then the local field potentials summate, and measurable voltage oscillations can be recorded in the electroencephalogram (EEG). These oscillations are observed over a wide range of frequencies and reflect the synchronous neuronal activity that occurs during a variety of different behaviors. For example, as animals explore their environments, as they learn and lay down memories, as they process sensory input, and as they sleep, characteristic oscillations occur in the ''theta'' range of frequencies (4–12 Hz) (1). These theta oscillations are often divided into two types (1–5): Type I, which occurs at slightly higher frequencies (6–12 Hz), and type II (also known as arousal theta), which occurs at the lower end of the range (4–9 Hz). Type I theta is associated with exploratory behavior, walking, running, and rearing, whereas type II theta is associated with immobility during the processing of sensory stimuli relevant to initiating, or intending to initiate, motor activity.

The neuronal networks that generate these theta oscillations involve ascending pathways from the brainstem that project to the hypothalamus and then to the medial septum/diagonal band of Broca and the hippocampus (6–9). Where the true pacemaker is located is unclear, but the basic requirements for a neuron to oscillate are a depolarizing drive (such as a sodium current) together with a restoring drive, such as a repolarizing potassium current. Most computational models (10–12) include several different ionic currents, some of which are well-characterized and attributed to known ion channels (e.g., HCN channels underlying I_h), whereas others are only defined operationally (e.g., slow potassium currents).

We have been studying the role TASK-3 potassium channels might play in general anesthesia. This channel is a member of a family of 15 ''background'' or ''leak'' potassium channels (13) that is directly inhibited by acid and activated by certain inhalational anesthetics (14, 15). During our initial experiments, we monitored the cortical EEG as a function of anesthetic concentration and made a striking observation. In wild-type mice, a highly-tuned anesthetic-induced peak in the theta band of frequencies (4–9 Hz), which appeared at around the concentrations that induced a loss of righting reflex, was absent in the TASK-3 knockout (KO) animals. TASK-1 KO mice, on the other hand, appeared identical to wild-type animals.

In this paper we show that the ablation of TASK-3 potassium channels removes type II theta oscillations, but leaves type I theta oscillations and exploratory behavior unaffected. Moreover, the TASK-3 KO mice show altered anesthetic sensitivity, disrupted sleep behavior, and a fragmentation of both sleep episodes and theta oscillations during REM sleep. These results suggest that TASK-3 channels play key roles in anesthetic sensitivity and the regulation of sleep.

Results

Anesthetic-Induced Loss of Righting Reflex. To assess any differences in anesthetic sensitivity between wild-type, TASK-1 KO, and TASK-3 KO animals, we used the loss of righting reflex (LORR) as an assay. In rodents, LORR is observed at the same concentrations as loss of consciousness in humans (16), with a comparably steep concentration-response curve reflecting a sharp transition between the awake and anesthetized states. We first investigated halothane because of its great efficacy in activating TASK channels (14, 15, 17–19). We found that the TASK-3 KO mice were significantly ($P < 0.001$) less sensitive to halothane, with an EC_{50} of $0.94 \pm 0.02\%$ atm ($n = 12$) compared with $0.68 \pm 0.02\%$ atm ($n = 19$) for wild-type animals (Fig. 1*A*). In contrast, TASK-1 KO mice showed only a small change in anesthetic sensitivity with an EC_{50} of $0.78 \pm 0.01\%$ atm; $n = 20$. To help assess if the difference between wild-type and TASK-3

Author contributions: S.G.B. and N.P.F. designed research; D.S.J.P., C.J.R., D.R.C., T.C.G., A.C., A.Y.Z., and N.P.F. performed research; A.L.V. and W.W. contributed new reagents/analytic tools; D.S.J.P., C.J.R., D.R.C., T.C.G., A.Y.Z., W.W., S.G.B., and N.P.F. analyzed data; and W.W. and N.P.F. wrote the paper.

The authors declare no conflict of interest.

This article is a PNAS Direct Submission.

Freely available online through the PNAS open access option.

[1]D.S.J.P. and C.J.R. contributed equally to this work.

[2]Present address: School of Pharmacy, University of London, 29/39 Brunswick Square, London WC1N 1AX, UK.

[3]To whom correspondence should be addressed. E-mail: n.franks@imperial.ac.uk.

www.pnas.org/cgi/doi/10.1073/pnas.0907228106

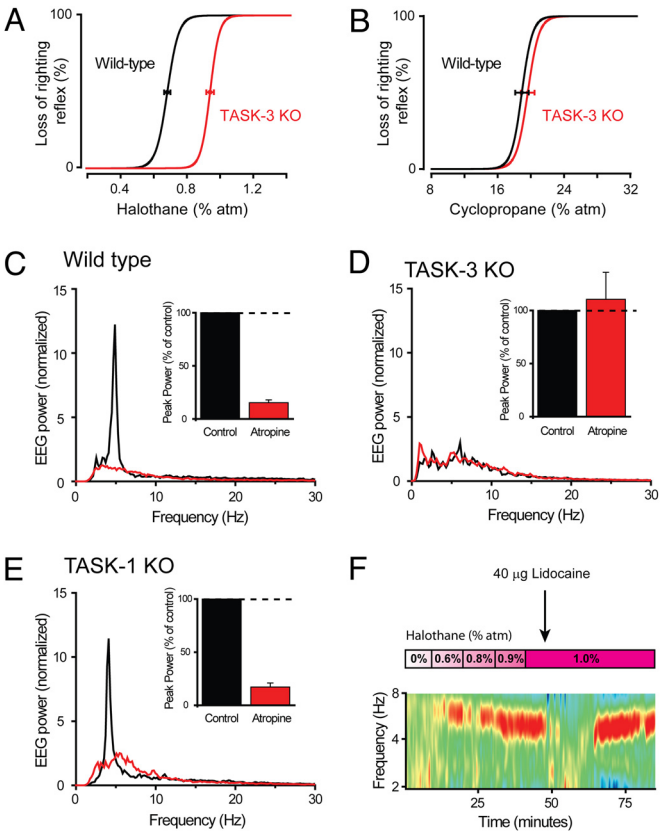

Fig. 1. The ablation of TASK-3 potassium channels alters anesthetic sensitivity and eliminates an atropine-sensitive theta oscillation. (*A*) TASK-3 KO mice are significantly ($P < 0.001$) less sensitive to halothane, an anesthetic that potently activates TASK channels (14, 17–19). (B) In contrast, the loss of righting reflex caused by cyclopropane, an anesthetic that has no effect on TASK-3 channels (20), was unchanged ($P > 0.5$). (*C*) At around loss of righting reflex concentrations, halothane induced a tuned oscillation in the EEG power spectrum in the theta band of frequencies in wild-type animals that was sensitive to atropine (*Inset*). (*D*) TASK-3 KO mice had a strikingly different phenotype. Halothane did not induce a tuned theta oscillation at any concentration. (*E*) TASK-1 KO mice displayed an identical behavior to wild-type animals, with halothane also inducing a tuned theta oscillation sensitive to atropine (see inset). The power spectra shown in panels *C–E* were all obtained in the presence of 1% halothane. (*F*) Injection of lidocaine into the medial septum reversibly inhibited the halothane-induced theta oscillation in wild-type mice. The Wavelet power spectrum shows the appearance of a theta oscillation during halothane exposure and its abrupt elimination, and then recovery, following lidocaine injection. Lidocaine injections were made on the midline at a depth from the surface of the skull of 5 mm and 0.8 mm from the Bregma.

KO animals was specifically due to the absence of TASK-3 channels, we next investigated the effects of cyclopropane, an anesthetic gas that, even at the highest concentrations, does not significantly activate TASK-3 channels (20). We found that for cyclopropane, the EC_{50} for LORR was identical ($P > 0.5$) for wild-type and TASK-3 KO animals, being 19.6 ± 0.8% atm ($n = 10$) and 19.0 ± 0.8% atm ($n = 12$), respectively (Fig. 1*B*).

An Atropine-Sensitive Theta Oscillation Is Absent in TASK-3 KO Mice. In parallel with our LORR measurements, we recorded the cortical EEG as a function of anesthetic concentration. In wild-type animals, we observed the striking appearance of a highly tuned peak in the theta range of frequencies (≈4–9 Hz) in the power spectrum when the mice were exposed to halothane at and above the concentrations that caused a LORR (Fig. 1*C*). In contrast, this peak was absent in TASK-3 KO animals (Fig. 1*D*). We obtained the same results with another inhalational general anesthetic, isoflurane ($n = 4$). In wild-type animals, this halothane-induced theta oscillation could be greatly (≈85%) inhibited ($n = 3$) by systemic atropine (50 mg/kg i.p.), a nonselective antagonist of muscarinic acetylcholine receptors (inset to Fig. 1*C*). The same dose of atropine had no significant effect ($n = 6$) on the power spectra from TASK-3 KO mice in the presence of halothane (Fig. 1*D*) or on the power spectra from wild-type ($n = 3$) or TASK-3 KO ($n = 7$) mice in the absence of halothane. We also performed the above experiments using TASK-1 KO mice and found identical results ($n = 4$) to those using wild-type animals (e.g., see Fig. 1*E*).

Atropine-sensitive theta oscillations (sometimes called type II theta oscillations) that are resistant to the presence of anesthetics are mediated by GABAergic and cholinergic projections from the medial septum to the hippocampus (21, 22). To confirm that this septohippocampal pathway was involved, we injected ($n = 3$) the local anesthetic lidocaine into the medial septum in wild-type mice exposed to a concentration of halothane sufficient to induce the sharply tuned theta oscillation. Lidocaine injection caused an abrupt and almost complete elimination of the theta peak; the effect reversed after about 20 min. This is illustrated by the data of Fig. 1*F*, which shows the Wavelet power spectrum (see *Materials and Methods*) of the EEG as a function of time, just before, and following, lidocaine injection in the presence of halothane. The involvement of cholinergic pathways is also suggested by the fact that anticholinesterase drugs such as physostigmine produce slow type II theta oscillations in many species, including mice (23–25). We confirmed this in wild-type mice ($n = 3$) and found that an i.p. injection of 0.2 mg/kg produced a 270 ± 60% increase ($P < 0.05$) in peak theta power centered at 4.5 Hz. In TASK-3 KO animals, in contrast, this dose of physostigmine had no significant effect ($n = 3$; $P > 0.1$).

We next examined how the theta oscillation was influenced by halothane concentration. For all three genotypes (wild-type, TASK-1 KO, and TASK-3 KO), a peak in the theta range was observed at low halothane concentrations (typically between 7–8 Hz), but this gradually shifted to lower frequencies as the concentration of halothane increased (Fig. 2 *A–C*). With both wild-type ($n = 8$) and TASK-1 KO ($n = 6$) mice, the peak sharpened and the peak power greatly increased, reaching a maximum at around 1% halothane. This is shown in Fig. 2 *D* and *E* where the "Quality"-factor Q (defined as the peak frequency/peak width) is plotted against anesthetic concentration. The Q-factor is a measure of the "tuning" of the oscillation. For TASK-3 KO mice ($n = 11$), this tuned, atropine-sensitive, theta oscillation was absent (Fig. 2*F*).

Cyclopropane, which is inactive on TASK-3 channels, caused no significant increase in theta power for either wild-type ($n = 7$) or TASK-3 KO animals ($n = 8$) over the range of concentrations tested (8–25% atm).

Exploratory Theta Oscillations in Wild-Type and TASK-3 KO Animals Are Identical. Theta oscillations occur when animals explore their environments (1, 5, 26), and we next investigated how this "exploratory" or type I theta was affected by the TASK-3 potassium channel ablation and the absence of type II theta. Mice were placed in an activity monitor so that their walking speed could be recorded at the same time as their EEG. The FFT power spectra were essentially identical for the wild-type and TASK-3 KO animals (Fig. 3*A*). However, because it has been reported (27–30) that the frequency of the exploratory theta oscillations increases with the speed of the animal, we investigated whether or not this occurred in our mice. Because of the limitations of conventional power spectra in terms of time/frequency resolution, we calculated the Wavelet power spectrum (31) as a function of time (Fig. 3*B*) and, using the coordinates provided by the activity monitor, calculated the frequency at

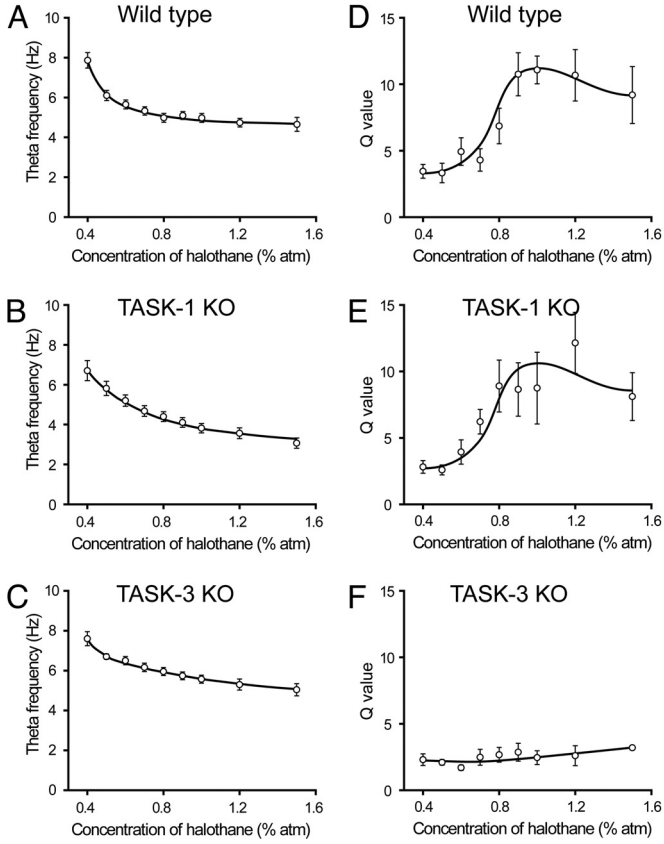

Fig. 2. Characteristics of theta oscillations in the presence of halothane for wild-type, TASK-1, and TASK-3 KO animals. Halothane caused a concentration-dependent decrease in theta frequency in (*A*) wild-type mice, (*B*) TASK-1 KO mice, and (*C*) TASK-3 KO mice. For both (*D*) wild-type and (*E*) TASK-1 KO animals, however, this was accompanied by a marked increase in peak theta power and the sharpness of the theta peak at and above the concentrations that induce a loss of righting reflex. This is shown by the plots of the Q-factor vs. halothane concentration. The Q-factor of a tuned oscillator is defined as the frequency divided by the full width at half maximum. (*F*) With TASK-3 KO mice, halothane did not increase theta power, and the Q-factor did not change significantly with halothane concentration.

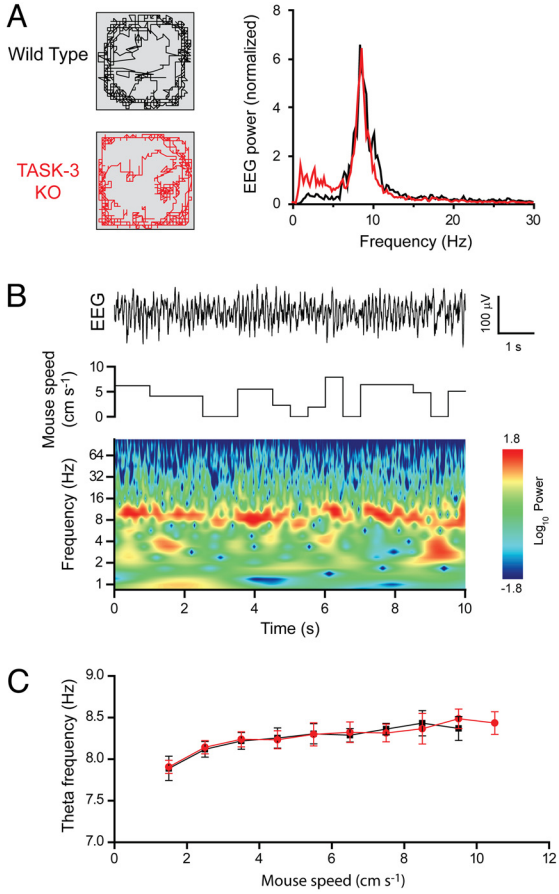

Fig. 3. The theta oscillations that occur when mice explore their environments, ''exploratory theta,'' were identical in wild-type and TASK-3 KO mice. (*A*) The Fast Fourier Transform (FFT) power spectrum of the EEG for mice moving at >2.5 cm/s showed a clear peak at around 8 Hz, which was essentially identical in wild-type and TASK-3 KO mice. On the left are typical traces showing the movement of the different genotypes over a 30-min period—as with the FFT power spectra, no differences were evident in the activities of the mice. (*B*) The top traces show a typical segment of the EEG for a wild-type mouse with the corresponding speed of the animal averaged over 0.5-s epochs. The Wavelet power spectrum (see *Material and Methods*) beneath shows how the frequency content of the EEG changes with time and illustrates how trains of theta oscillations (at ≈8 Hz) are often interrupted when the animal stops moving. (*C*) A more detailed analysis reveals that the frequency at peak theta power shows a significant increase ($P < 0.05$, repeated measures ANOVA) as a function of the speed of the animal.

maximum theta power as a function of the speed of the mouse. The data confirmed that the theta frequency does, indeed, increase with the speed of the animal, but the data for wild-type ($n = 5$) and TASK-3 KO ($n = 5$) animals were virtually identical (Fig. 3*C*). These data also serve to emphasize that the absence of TASK-3 channels has selectively ablated one specific type of theta oscillation.

Natural Sleep and Theta Oscillations During REM Are Fragmented in TASK-3 KO Animals. Given that network oscillations feature prominently in sleep and that TASK-3 KO mice are more active during the nocturnal period (32), we next investigated if the natural sleep behavior of the mice had been affected. By using miniature data-logging devices, we recorded the EEG and EMG of mice in their ''natural'' home-cage environments over the full sleep-wake cycle. There was a clear distinction in sleep behavior between the genotypes (Fig. 4*A*). As expected, wild-type animals (black lines in Fig. 4*A*, $n = 5$) showed a large difference ($n = 5$) in the levels of wakefulness, non-REM and REM sleep during the ''lights on'' 12-h period (natural sleep period) compared with the ''lights off'' period (natural wake period). Moreover, the progression between these different behavioral states was rather abrupt. The TASK-3 KO animals ($n = 5$), on the other hand, showed a much slower progression when moving from the natural wake period to the sleep period. During the first 2 h after ''lights on,'' the TASK-3 KO animals spent significantly ($P < 0.05$) more time awake, and significantly ($P < 0.05$) less time in REM or non-REM, than wild-type mice, but this difference progressively reduced over time.

When the distributions of sleep episodes were analyzed, we found that, during the natural wake period, the number and average length of sleep episodes was not significantly different ($P > 0.1$ and $P > 0.5$, respectively) for wild-type and TASK-3 KO mice (Fig. 4*B*, top graph). In contrast, there was an obvious difference between the genotypes during the natural sleep period. Here, the number of sleep episodes for the TASK-3 KO mice was significantly ($P < 0.001$) larger than for the wild-type (36.0 ± 3.5 compared with 19.3 ± 2.5), but their durations were significantly ($P < 0.005$) shorter (655 ± 52 s compared with 1452 ± 180 s). In other words, the sleep episodes were fragmented.

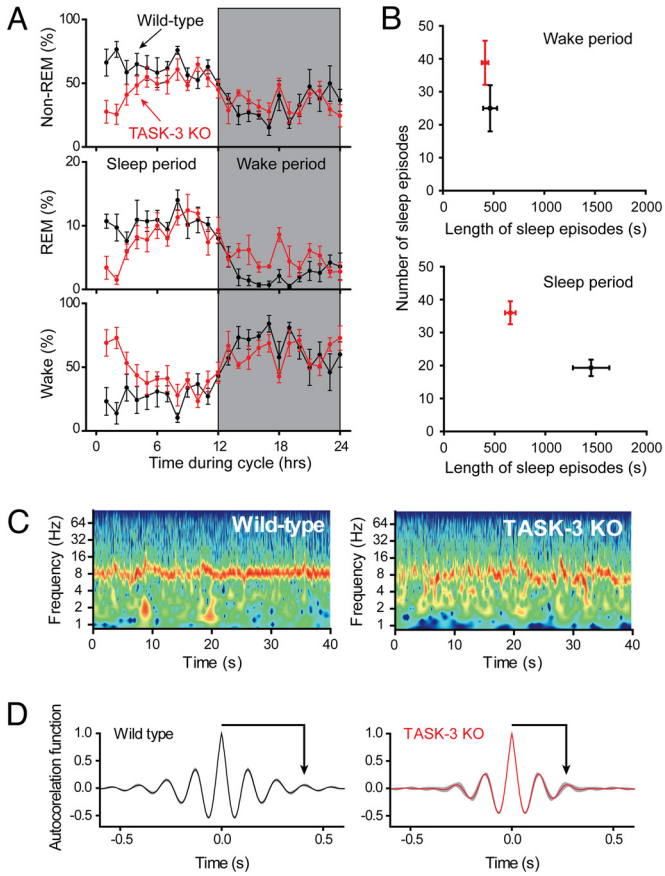

Fig. 4. The ablation of TASK-3 channels disrupts natural sleep and fragments both sleep episodes and theta oscillations. (*A*) TASK-3 KO mice show a much slower progression into sleep (both into non-REM and REM) at the start of the natural sleep period (''lights on''). During the natural wake period (''lights off'') the sleep behavior of the two genotypes is broadly similar. (*B*) The upper panel shows that there were no significant differences in sleep fragmentation during the natural wake period. During the natural sleep period (lower panel), however, the TASK-3 KO animals show a fragmented sleep pattern with significantly more ($P < 0.001$), but significantly shorter ($P < 0.005$) sleep episodes. (*C*) REM sleep episodes during the natural sleep period showed a clear difference in the fragmentation of the theta oscillations. The Wavelet power spectra show illustrative examples of 40-s segments of EEG during REM for wild-type and TASK-3 KO mice. The autocorrelations in (*D*) reflect this quantitatively and show that the wild-type mice ($n = 5$) display more coherent REM theta oscillations ($P < 0.05$) than do TASK-3 KO mice ($n = 5$). The gray shading represents the SEM envelope, and the arrows indicate the time at which a peak in the autocorrelation function is no longer significantly different from zero.

Because the most striking phenotypic difference between the wild-type and TASK-3 KO animals was the loss of the type II theta oscillations (Fig. 1 *C* and *D*), and because natural sleep had been disrupted, we next investigated whether the theta oscillations that occur during REM sleep were also affected. We calculated the Wavelet power spectrum as a function of time during periods of sustained REM sleep that occurred during the natural sleep period (''lights on''). Increased fragmentation of the theta oscillations was evident in the Wavelet power spectra of the TASK-3 KO mice. Fig. 4*C* shows representative examples of Wavelet power spectra for the two genotypes, where it can be seen that in wild-type animals, theta oscillations tend to be less interrupted. This is shown quantitatively by the autocorrelation functions shown below (Fig. 4*D*) calculated on 120-s segments of data from both wild-type (left graph; $n = 5$) and TASK-3 KO animals (right graph; $n = 5$). A test between the peak heights in the autocorrelation functions show a significant difference ($P < 0.05$) between the wild-type and KO animals.

Discussion

The TASK-3 KO mice were significantly less sensitive to the general anesthetic halothane. Indeed, they showed the greatest genetically-engineered decrease in sensitivity to an inhalational anesthetic yet reported for anesthetic-induced hypnosis (16, 33). This decrease in halothane sensitivity is comparable with that observed with TREK-1 KO mice in response to a painful stimulus (33). The fact that the TASK-3 KO mice displayed an unchanged sensitivity to cyclopropane, an agent that does not measurably activate TASK-3 channels (20), supports the idea that the decrease in halothane sensitivity was a direct consequence of their absence. Thus, involvement of TASK-3 channels in anesthetic-induced LORR seems likely. A possible role for anesthetic-activated potassium channels was suggested many years ago (34). The first such channel that was characterized was discovered in the pond snail *Lymnaea stagnalis* (18), and when recently cloned (17), found to be closely related to mammalian TASK channels that have been shown to be activated by a variety of volatile general anesthetics (14, 15). Nonetheless, other channels, such as $GABA_A$ receptors and other two-pore-domain potassium channels are almost certain to be involved (16, 35, 36), because at only 40% higher concentrations, the TASK-3 KO mice are also anesthetized.

The loss of type II theta oscillations in the TASK-3 KO mice was completely unexpected. This theta oscillation has been widely studied, using a variety of different anesthetics (4, 6, 8, 37). The increased tuning of the oscillation under halothane anesthesia implies that the opening of TASK-3 channels promotes neuronal synchronicity. The oscillation is characterized by its sensitivity to atropine, and it has been postulated to mediate the processing of sensory stimuli before initiating motor activity (2–5). The absence of type II theta was specific to the loss of the TASK-3 channels, because the removal of TASK-1 channels left the oscillations unchanged.

Our finding that type I exploratory theta oscillations are identical in the wild-type and TASK-3 KO animals has important implications for the extent to which the pathways and molecular mechanisms that mediate the two types of theta oscillations overlap. Clearly, TASK-3 potassium channels are a necessary component for type II oscillations but play no evident role in type I oscillations. Although the circuitry responsible for generating these oscillations is not certain, it is widely believed that a pathway from the brainstem, ascending through the hypothalamus to the medial septum and hippocampus is involved (1, 6–9). This is consistent with our observation that the type II theta oscillation can be reversibly blocked by lidocaine injection into the medial septum.

Given that the recombinant TASK-1 and TASK-3 channels have similar biophysical properties with respect to anesthetic sensitivity (15), why are the deficits in oscillatory activity and sleep patterns specific to the TASK-3 KO strain? This is probably because of differences in neuronal expression between the two genes (38); we surmise that the TASK-1 gene is not expressed, or not expressed highly, in the neurons either driving or supporting the oscillations. In the adult mouse forebrain the TASK-3 gene has much stronger expression than TASK-1. In particular, TASK-3 mRNA is abundant in layers 2 to 6 of the neocortex, CA1 hippocampal pyramidal cells, dentate granule cells, and the septum (38, 39); the TASK-3 gene is also expressed in parvalbumin-positive GABAergic interneurons (40) in the hippocampus, some subtypes of which aid the generation of theta oscillations (41, 42). The TASK-1 gene, by contrast, is poorly expressed in the mouse hippocampus (38). One scenario is that, as a consequence of losing TASK-3 channels, a change in the biophysical behavior of a specific type of hippocampal interneu-

ron (e.g., a subtype of parv-positive interneuron) might produce the selective loss of type II theta with minimal impact on type I theta. It has recently been shown, for example, that the loss of TASK-3 channels in cerebellar granule neurons affects their ability to sustain high-frequency firing of action potentials (43). Alternatively, TASK-3 channels might govern the regulation of selective cholinergic input to the hippocampus, so their absence might disrupt theta oscillations. More work is needed to elucidate the cellular mechanism.

Previously, establishing the physiological roles of type II theta oscillations has been problematic because they are only sustained when anesthetic is present, or can only be blocked when atropine is present. Both of these drug treatments will affect neuronal behavior in ways that do not involve theta oscillations per se. TASK-3 KO animals should allow us to test hypotheses about where and when these oscillations might play a role. Whether or not the theta oscillations that are elicited by various drug treatments correspond to the theta oscillations that are observed during specific behavioral states requires further investigation.

Network oscillations and sleep are intimately connected, with sleep states largely characterized by the frequency and amplitude of oscillations in the EEG. Transient spindles and K-complexes appear before sleep onset, and the relative amplitudes of theta and delta oscillations (together with the EMG) allow REM and non-REM sleep states to be distinguished. It is too early to be certain that the absence of type II theta oscillations in the TASK-3 KO animals is directly responsible for the changes we observe in sleep behavior. Nonetheless, the differences we see in both the time to transition into both REM and non-REM sleep, as well as the fragmentation in the sleep episodes are a strong indication that modulation of TASK-3 potassium channels is part of the mechanism used in natural sleep regulation, perhaps via muscarinic acetylcholine receptors (44). Interestingly, atropine treatment, which blocks type II theta oscillations, also shortens REM episodes in both cats (45) and rats (46). The fragmentation of the theta oscillations during REM episodes is further evidence of TASK-3 involvement in sleep mechanisms in general and theta oscillations in particular.

In summary, we have made the surprising discovery that TASK-3 channels are required for atropine-sensitive type II theta oscillations. In contrast, they make no contribution to type I exploratory theta oscillations. Animals lacking these channels display a reduced sensitivity to the general anesthetic halothane, have a significantly slower progression into sleep, and exhibit fragmented sleep behavior. Because of the many ways in which TASK-3 channels can be modulated, it is easy to imagine that this might lead to the regulation of behavior via the promotion or reduction of theta oscillations.

Materials and Methods

Mice. All experiments were in accordance with the United Kingdom Animals (Scientific Procedures) Act of 1986 and approved by the Ethical Review Committee of Imperial College London. Animals were housed in a humidity- and temperature-controlled room, under a 12:12-h light-dark cycle. Water and food were provided ad libitum. The TASK-1 (39) and TASK-3 KO (43) mice, each with a disruption of the first coding exon, were as described previously.

Anesthetic-Induced Loss of Righting Reflex. An animal was placed in a cylindrical glass chamber (900 mL) and, following a 10-min baseline period with 100% oxygen, the anesthetic was introduced, initially at 0.4% for halothane or 8% for cyclopropane. The anesthetic concentration was then increased stepwise (steps of 0.1% for halothane and 4% for cyclopropane), and after 10 min equilibration, LORR was assessed by manually rotating the glass cylinder and scoring a LORR if the animal had all four feet off the ground for 30 s or more. The observer was blinded to the genotype of the animal. Each animal was tested once at each anesthetic concentration. Normothermia was maintained using a heat lamp placed 45 cm above the glass cylinder. A quantal concentration-response curve was calculated using the method of Waud (47).

EEG Recording. Surgery was carried out under halothane (0.8–1.5% in oxygen) anesthesia. Three gold-plated EEG electrodes (Decolletage AG) were inserted through the skull onto the dura mater, the first in the frontal bone (+1.5 mm to Bregma, -1.5 mm from midline), the second in the parietal bone (−1.5 mm to Bregma, +1.5 mm from midline), and the third in the interparietal bone over the cerebellum (−2.0 mm from Lambda, 0.0 mm from midline) for the reference electrode. Three lengths of Teflon-insulated stainless steel wire (with the distal 3 mm of insulation removed) were inserted in the neck muscle for EMG recording. Once all of the electrodes were in place, they were covered with dental cement (Orthoresin; DeguDent GmbH). The animals were allowed at least 7 days to recover from surgery. The EEG and EMG signals were recorded on a miniature data logging device (48) containing a 256 MB memory chip (http://www.vyssotski.ch/neurologger2). This device was sufficiently small (about 2 g including batteries) to be attached directly to the animal's skull. Four data channels (up to 30 h at 10-bit resolution) could be recorded at a sampling rate of 400 Hz and were bandpass-filtered (−3 db corner frequency) between 1 and 70 Hz followed by high-pass (0.6 Hz, -3db) offline digital filtering. The recording device allowed EEG-EMG signals to be recorded in free-moving animals, either in an activity monitor or in their home cages, where data could be recorded during a complete sleep-wake cycle in a natural and familiar environment.

It should be noted that our EEG measurements were from the cortex, so that the sleep state of the mice could be determined. Previous work on theta oscillations has usually been done with rats, often using hippocampal electrodes. However, because of the small distance between the hippocampus and the cortex in mice, it is almost certain that oscillations generated in the hippocampus would be detected by our cortical EEG electrodes.

EEG Analysis. EEG data were analyzed using either conventional FFT power spectra (Fast Fourier transforms of the autocorrelation function) or Morlet Wavelet analysis. FFT power spectra were calculated using the program Spike (Spike 2, v5.14; Cambridge Electronic Design) with the area being normalized to 100. Where a theta peak was observed, a good fit to the data could be obtained using a Lorentzian function:

$$p = p_0 + \left\{ \frac{a_0 \gamma^2}{\gamma^2 + (f - f_0)^2} \right\}$$

where p is the EEG power, p_0 is a baseline, a_0 is the height of the Lorenzian, γ is the half-width at half maximum, f is the frequency and f_0 is the peak frequency. The Q-factor, a measure of the sharpness of the peak, was calculated as $f_0/(2\gamma)$.

EEG data were also analyzed using Wavelet transforms (49), which are appropriate when the EEG signal is nonstationary (which is often the case); the Wavelet power spectrum is the square of the Wavelet transform. This method involves convoluting the EEG signal with a series of ''Daughter'' wavelets, which are time-scaled variants of a ''Mother'' wavelet. In general, the wavelet transform is defined as:

$$W(s, \tau) = \frac{1}{\sqrt{s}} \int x(t)\ \psi\left(\frac{t - \tau}{s}\right) dt$$

where s and τ represent the scale and local center of the wavelet $\psi(s, \tau)$, and $x(t)$ is the EEG signal as a function of time. We used the most commonly used Mother wavelet, the Morlet function, which is a complex sinusoid, windowed by a Gaussian:

$$\psi_0(\eta) = \pi^{-1/4} e^{i\omega_0 \eta} e^{-\eta^2/2}$$

where η is a dimensionless ''time'' parameter, and ω_0 is the dimensionless wavelet central ''frequency'' that was set to 6 to satisfy the admissibility criterion (50). The Wavelet power spectra were calculated using Matlab (MathWorks) using a script based on that of Torrence and Compo (49).

Sleep Scoring. For the sleep experiments, mice were placed in a temperature-controlled, sound-proof box illuminated within on a 12:12-h light-dark cycle. Data were recorded both from animals in their home cages as well as from animals exposed to a novel environment (an activity test chamber). In these latter experiments, as well as the EEG-EMG signals, the coordinates of the animal were recorded using two orthogonal sets of 16 infrared beams (Activity test chamber; Med Associates) and analyzed with Activity Monitor software (Med Associates). The activity box was thoroughly cleaned with ethanol between experiments.

The sleep state (rapid-eye-movement sleep, REM; nonrapid-eye-movement sleep, non-REM; or wake, W) was scored automatically using an established

protocol (51). Briefly, the scoring consisted of filtering the EEG into ''delta'' (0.5–4 Hz) and ''theta'' (6–10 Hz) frequency bands and scoring 20-s epochs as one or other of the three states based on W being periods of high EMG and intermediate theta/delta ratio, REM being periods with high theta/delta ratio and low EMG and non-REM being periods with high delta waves, low theta/delta ratio, and low EMG.

Statistics. Unless otherwise stated, Student's *t*-test was used to test for significance. Where shown, errors bars represent the SEM.

ACKNOWLEDGMENTS. We thank Raquel Yustos for technical assistance and Geoff Horseman (CED Ltd.) for help with the sleep-scoring algorithm. C.J.R. held a studentship from the Medical Research Council (UK); D.S.J.P. was the recipient of a studentship from the Royal College of Anesthetists and the British Journal of Anesthesia; and A.C., D.R.C., and T.C.G. were recipients of studentships from the Biotechnology and Biological Sciences Research Council (UK). This work was supported by grants from the Biotechnology and Biological Sciences Research Council G021691; Air Products and Chemicals, Inc.; and Medical Research Council (UK) Grant G0501584 (to N.P.F., S.G.B., and W.W.).

1. Buzsaki G (2002) Theta oscillations in the hippocampus. *Neuron* 33:325–340.
2. Oddie SD, Kirk IJ, Whishaw IQ, Bland BH (1997) Hippocampal formation is involved in movement selection: Evidence from medial septal cholinergic modulation and concurrent slow-wave (theta rhythm) recording. *Behav Brain Res* 88:169–180.
3. Vanderwolf CH (1969) Hippocampal electrical activity and voluntary movement in the rat. *Electroencephalogr Clin Neurophysiol* 26:407–418.
4. Kramis R, Vanderwolf CH, Bland BH (1975) Two types of hippocampal rhythmical slow activity in both the rabbit and the rat: Relations to behavior and effects of atropine, diethyl ether, urethane, and pentobarbital. *Exp Neurol* 49:58–85.
5. Oddie SD, Bland BH (1998) Hippocampal formation theta activity and movement selection. *Neurosci Biobehav Rev* 22:221–231.
6. Colom LV, et al. (1991) In vivo intrahippocampal microinfusion of carbachol and bicuculline induces theta-like oscillations in the septally deafferented hippocampus. *Hippocampus* 1:381–390.
7. Kirk IJ (1998) Frequency modulation of hippocampal theta by the supramammillary nucleus, and other hypothalamo-hippocampal interactions: Mechanisms and functional implications. *Neurosci Biobehav Rev* 22:291–302.
8. Kirk IJ, McNaughton N (1993) Mapping the differential effects of procaine on frequency and amplitude of reticularly elicited hippocampal rhythmical slow activity. *Hippocampus* 3:517–525.
9. Vertes RP, Kocsis B (1997) Brainstem-diencephalo-septohippocampal systems controlling the theta rhythm of the hippocampus. *Neuroscience* 81:893–926.
10. Acker CD, Kopell N, White JA (2003) Synchronization of strongly coupled excitatory neurons: Relating network behavior to biophysics. *J Comput Neurosci* 15:71–90.
11. Rotstein HG, et al. (2005) Slow and fast inhibition and an H-current interact to create a theta rhythm in a model of CA1 interneuron network. *J Neurophysiol* 94:1509–1518.
12. Traub RD, et al. (2004) Cellular mechanisms of neuronal population oscillations in the hippocampus in vitro. *Annu Rev Neurosci* 27:247–278.
13. Goldstein SA, Bockenhauer D, O'Kelly I, Zilberberg N (2001) Potassium leak channels and the KCNK family of two-P-domain subunits. *Nat Rev Neurosci* 2:175–184.
14. Patel AJ, et al. (1999) Inhalational anesthetics activate two-pore-domain background K^+ channels. *Nat Neurosci* 2:422–426.
15. Talley EM, Bayliss DA (2002) Modulation of TASK-1 (Kcnk3) and TASK-3 (Kcnk9) potassium channels: Volatile anesthetics and neurotransmitters share a molecular site of action. *J Biol Chem* 277:17733–17742.
16. Franks NP (2008) General anaesthesia: From molecular targets to neuronal pathways of sleep and arousal. *Nat Rev Neurosci* 9:370–386.
17. Andres-Enguix I, et al. (2007) Determinants of the anesthetic sensitivity of two-pore domain acid-sensitive potassium channels: Molecular cloning of an anesthetic-activated potassium channel from *Lymnaea stagnalis*. *J Biol Chem* 282:20977–20990.
18. Franks NP, Lieb WR (1988) Volatile general anaesthetics activate a novel neuronal K^+ current. *Nature* 333:662–664.
19. Lopes CMB, Franks NP, Lieb WR (1998) Actions of general anaesthetics and arachidonic acid pathway inhibitors on K^+ currents activated by volatile anaesthetics and FMRF-amide in molluscan neurones. *Br J Pharmacol* 125:309–318.
20. Gruss M, et al. (2004) Two-pore-domain K^+ channels are a novel target for the anesthetic gases xenon, nitrous oxide, and cyclopropane. *Mol Pharmacol* 65:443–452.
21. Mizumori SJ, Barnes CA, McNaughton BL (1989) Reversible inactivation of the medial septum: Selective effects on the spontaneous unit activity of different hippocampal cell types. *Brain Res* 500:99–106.
22. Oddie SD, Stefanek W, Kirk IJ, Bland BH (1996) Intraseptal procaine abolishes hypothalamic stimulation-induced wheel-running and hippocampal theta field activity in rats. *J Neurosci* 16:1948–1956.
23. Leung LS, Vanderwolf CH (1980) Behavior-dependent evoked potentials in the hippocampal CA1 region of the rat. II. Effect of eserine, atropine, ether and pentobarbital. *Brain Res* 198:119–133.
24. Bland BH, Colom LV (1988) Responses of phasic and tonic hippocampal theta-on cells to cholinergics: Differential effects of muscarinic and nicotinic activation. *Brain Res* 440:167–171.
25. Tebano MT, et al. (1999) Effects of cholinergic drugs on neocortical EEG and flash-visual evoked potentials in the mouse. *Neuropsychobiology* 40:47–56.
26. O'Keefe J (1993) Hippocampus, theta, and spatial memory. *Curr Opin Neurobiol* 3:917–924.
27. Jeewajee A, Barry C, O'Keefe J, Burgess N (2008) Grid cells and theta as oscillatory interference: Electrophysiological data from freely moving rats. *Hippocampus* 18:1175–1185.
28. Rivas J, Gaztelu JM, Garcia-Austt E (1996) Changes in hippocampal cell discharge patterns and theta rhythm spectral properties as a function of walking velocity in the guinea pig. *Exp Brain Res* 108:113–118.
29. Slawinska U, Kasicki S (1998) The frequency of rat's hippocampal theta rhythm is related to the speed of locomotion. *Brain Res* 796:327–331.
30. Gordon JA, Lacefield CO, Kentros CG, Hen R (2005) State-dependent alterations in hippocampal oscillations in serotonin 1A receptor-deficient mice. *J Neurosci* 25:6509–6519.
31. Daubechies I (1990) The wavelet transform, time-frequency localization and signal analysis. *IEEE Trans Inf Theory* 36:961–1005.
32. Linden AM, et al. (2007) TASK-3 knockout mice exhibit exaggerated nocturnal activity, impairments in cognitive functions, and reduced sensitivity to inhalation anesthetics. *J Pharmacol Exp Ther* 323:924–934.
33. Heurteaux C, et al. (2004) TREK-1, a K^+ channel involved in neuroprotection and general anesthesia. *EMBO J* 23:2684–2695.
34. Nicoll RA, Madison DV (1982) General anesthetics hyperpolarize neurons in the vertebrate central nervous system. *Science* 217:1055–1057.
35. Hemmings HC, Jr, et al. (2005) Emerging molecular mechanisms of general anesthetic action. *Trends Pharmacol Sci* 26:503–510.
36. Rudolph U, Antkowiak B (2004) Molecular and neuronal substrates for general anaesthetics. *Nat Rev Neurosci* 5:709–720.
37. Bland BH, et al. (2003) Effect of halothane on type 2 immobility-related hippocampal theta field activity and theta-on/theta-off cell discharges. *Hippocampus* 13:38–47.
38. Aller MI, Wisden W (2008) Changes in expression of some two-pore domain potassium channel genes (KCNK) in selected brain regions of developing mice. *Neuroscience* 151:1154–1172.
39. Aller MI, et al. (2005) Modifying the subunit composition of TASK channels alters the modulation of a leak conductance in cerebellar granule neurons. *J Neurosci* 25:11455–11467.
40. Torborg CL, et al. (2006) TASK-like conductances are present within hippocampal CA1 stratum oriens interneuron subpopulations. *J Neurosci* 26:7362–7367.
41. Klausberger T, Somogyi P (2008) Neuronal diversity and temporal dynamics: The unity of hippocampal circuit operations. *Science* 321:53–57.
42. Wulff P, et al. (2009) Hippocampal theta rhythm and its coupling with gamma oscillations require fast inhibition onto parvalbumin-positive interneurons. *Proc Natl Acad Sci USA* 106:3561–3566.
43. Brickley SG, et al. (2007) TASK-3 two-pore domain potassium channels enable sustained high-frequency firing in cerebellar granule neurons. *J Neurosci* 27:9329–9340.
44. Meuth SG, et al. (2003) Contribution of TWIK-related acid-sensitive K^+ channel 1 (TASK1) and TASK3 channels to the control of activity modes in thalamocortical neurons. *J Neurosci* 23:6460–6469.
45. Drucker-Colin R, et al. (1983) Dissociation of rapid eye movement (REM) sleep features: Possible implications for REM triggering mechanisms. *J Neurosci Res* 9:425–435.
46. Mavanji V, Datta S (2002) Sleep-wake effects of yohimbine and atropine in rats with a clomipramine-based model of depression. *Neuroreport* 13:1603–1606.
47. Waud DR (1972) On biological assays involving quantal responses. *J Pharmacol Exp Ther* 183:577–607.
48. Vyssotski A, et al. (2009) EEG responses to visual landmarks in flying pigeons. *Curr Biol* 19:1159–1166.
49. Torrence C, Compo G (1998) A practical guide to wavelet analysis. *Bull Amer Meteor Soc* 79:61–78.
50. Farge M (1992) Wavelet transforms and their applications to turbulence. *Annu Rev Fluid Mech* 24:395–457.
51. Costa-Miserachs D, Portell-Cortes I, Torras-Garcia M, Morgado-Bernal I (2003) Automated sleep staging in rat with a standard spreadsheet. *J Neurosci Methods* 130:93–101.